Journal of Power Sources 193 (2009) 483–487

Contents lists available at ScienceDirect

Journal of Power Sources

journal homepage: www.elsevier.com/locate/jpowsour

Short communication

A novel cesium hydrogen sulfate–zeolite inorganic composite electrolyte membrane for polymer electrolyte membrane fuel cell application

Jinhua Piao, Shijun Liao*, Zhenxing Liang

School of Chemistry and Chemical Engineering, South China University of Technology, Guangdong, Guangzhou 510640, China

ARTICLE INFO

Article history:
Received 4 March 2009
Received in revised form 9 April 2009
Accepted 10 April 2009
Available online 18 April 2009

Keywords:
Fuel cells
Solid acid
Electrolyte
Proton conductivity
Zeolite

ABSTRACT

A new type of $CsHSO_4$–HZSM-5 inorganic composite electrolyte membrane is prepared by mechanically mixing $CsHSO_4$ (CHS) and nanometer-scale HZSM-5 zeolite powders. The effects of HZSM-5 on the crystallite structure, proton conductivity, and thermal stability of the $CsHSO_4$ electrolyte are investigated. Incorporation of HZSM-5 is found to significantly increase the low-temperature proton conductivity of the $CsHSO_4$ electrolyte, extending its operating temperature down to 100 °C. The composite electrolyte with 40 mol% HZSM-5 shows the highest proton conductivity in the measured temperature range. The low-temperature activation energy of the composite with 40 mol% HZSM-5 is lower than that of the CHS–SiO_2 composite. The improvement of the proton conductivity can be attributed to the enhanced interfacial interaction between the two phases. And the small HZSM-5 particles lead to a change in the bulk properties of the ionic salts. The melting point of the CHS–HZSM-5 composite electrolyte is lower than that of the pure CHS electrolyte. The CHS–HZSM-5 composite electrolyte is suitable for polymer electrolyte membrane fuel cells operated at 100–200 °C.

1. Introduction

The development of novel proton-conducting solid electrolytes working at intermediate temperatures (100–300 °C) is currently considered an alternative way to solve the problems encountered in the present Nafion®-based low-temperature polymer electrolyte membrane fuel cells (PEMFCs) [1,2]. Solid acid compounds like $CsHSO_4$ (CHS) undergoing a superprotonic phase transition at an intermediate temperature (T_{tr} = 141 °C) could be used as the fuel cell electrolyte in the temperature range of 150–180 °C (melting point: 212 °C) [3]. Although this particular superprotonic solid acid shows excellent proton transport properties, it has not been considered for fuel cell applications due to its significant water solubility and inferior mechanical properties. Recently, since Haile et al. [4] reported the first examination of $CsHSO_4$ (CHS) as an electrolyte for PEMFC applications, other significant efforts in the community of fuel cell researchers have been devoted to studying this material.

As mentioned above, $CsHSO_4$ offers the advantages of anhydrous proton transport and high-temperature stability, which are highly desirable for the application of high-temperature PEMFCs [4]. However, $CsHSO_4$ shows poor proton conductivity when the temperature is below 141 °C, and it has been proven that $CsHSO_4$ transforms from a monoclinic to a tetragonal structure at 141 °C, with the proton conductivity steeply increasing by about 2–3 orders of magnitude during this transition. Therefore, the applicable operating temperature of the CHS electrolyte is restricted to a narrow range: from 140 °C to its melting temperature of about 210 °C. For the practical operation of fuel cells, high proton conductivity in a wide temperature range (100–200 °C) is highly desirable for electrolyte membranes [5]. Therefore, increasing the low-temperature proton conductivity of $CsHSO_4$ is very important from a practical point of view.

Heterogeneous doping of ionic salts with highly dispersed oxides has been shown to be an effective way to increase the conductivity at low and intermediate temperatures by transforming these salts into disordered systems [6,7]. Two-phase composites obtained by doping consist of an ionic conductor and a highly dispersed inert isolator, such as Al_2O_3, SiO_2, TiO_2, ZrO_2, MgO etc. [8]. New unusual disordered states of ionic salts may form at the interface due to the strong interaction between the components in nanocomposites and, the formation of such states depends on the chemical nature and concentration of the composite components, as well as the morphological character and the energy change of the interface interaction [9]. Ponomareva and Lavrova [9] doped the heterogeneous porous structure materials into $CsHSO_4$ electrolyte and found that the proton conductivity of composite is significantly increased by 1–3.5 orders of magnitude at low temperatures. The microstructure analyses showed broadened XRD diffraction peaks as well as obvious shifted, broadened, and even vanished DTA peaks, indicating that part of the CHS proton-conducting phase in the composites was present as an amorphous phase in the composite. It was also found that the conductivity and thermal

* Corresponding author. Fax: +86 20 87113586 608.
E-mail address: chsjliao@scut.edu.cn (S. Liao).

0378-7753/$ – see front matter © 2009 Elsevier B.V. All rights reserved.
doi:10.1016/j.jpowsour.2009.04.010

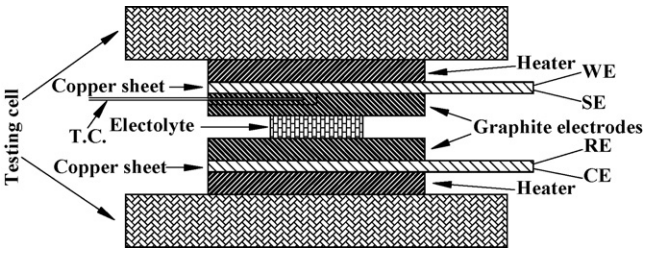

Fig. 1. Two-electrode setup for conductivity measurement.

stability of $(1-x)CsHSO_4$–xA composites increased in the order of $Al_2O_3 < TiO_2 < SiO_2$. Wang et al. [1] prepared $CsHSO_4$–SiO_2 composite membranes by heating CHS powder and SiO_2 membranes at 220–240 °C, at which the molten CHS was infiltrated into the SiO_2 membranes. The results showed that the nanocomposite with 4-nm pores in the original SiO_2 membrane exhibited a greater enhancement in the proton conductivity than that with 29-nm pores in the low-temperature range. In almost all of the proton or ion conducting nanocomposites prepared by the powder-mixing method, the protonic or ionic conducting phase is present in both bulk and interface phases. Therefore, the structure generated by heterogeneous doping of ionic salts is important in determining the composite properties.

Microporous HZSM-5 zeolite materials possess high specific surface area and strong acidity, which are beneficial for ionic transfer. Therefore, better performance of the electrolyte materials can be possibly obtained by doping the nanometer HZSM-5 zeolite materials into the $CsHSO_4$ materials. In the present work, we investigated the crystal structure, proton conductivity, and thermal stability of a composite electrolyte made of CHS and HZSM-5 powders (including different Si/Al ratios). The preliminary experimental results indicated that the low-temperature conductivity of CHS was significantly improved by doping with HZSM-5 materials.

2. Experimental

$CsHSO_4$ powders were prepared from an aqueous solution of cesium sulfate and sulfuric acid as follows. Cs_2SO_4 (Shanghai Jingchun Chemical Reagent Co., Ltd.) was first dissolved in dilute sulfuric acid (Guangzhou DongHong Chemical Plant) solution with the molar ratio of Cs_2SO_4:H_2SO_4:H_2O being 1:2:12. After the complete dissolution of Cs_2SO_4, ethanol was added into the solution to induce the precipitation of $CsHSO_4$. The precipitate was then filtered, dried at 100 °C overnight, and stored in a vacuum desiccator before further characterization [10–12]. For the test, the prepared $CsHSO_4$ powders were mixed with nanometer HZSM-5 (Si/Al = 35 and 300, Nankai University Catalyst Co., Ltd.) at various molar ratios and pressed into pellets of 1.5 cm diameter and 1–1.5 mm thickness. The samples were heated for 30 min at 210 °C (close to the melting point).

The crystal structure of the prepared CHS powders and CHS–HZSM-5 (Si/Al = 35) composite electrolytes was characterized with X-ray diffraction (XRD) (Shimadzu XD-3A, Japan) using Cu Kα radiation. Thermogravimetric analysis and differential thermal analyses (TG-DTA) were characterized with a NETZSCH STA 449C instrument at a heating rate of 10 °C min^{-1} from room temperature to 600 °C. The proton conductivity of $(1-x)CsHSO_4$–xHZSM-5 (x = 0–0.8 for Si/Al = 35 and x = 0.4 for Si/Al = 300) composite electrolytes was measured by AC impedance spectroscopy with an IM6e impedance spectroscopy instrument unit across the frequency range of 1 Hz to 100 kHz at an amplitude of 5 mV. A two-electrode setup was used to measure the proton conductivity (Fig. 1). The graphite electrodes were attached to both sides of the electrolyte pellets by pressing them against the testing cell. The composite

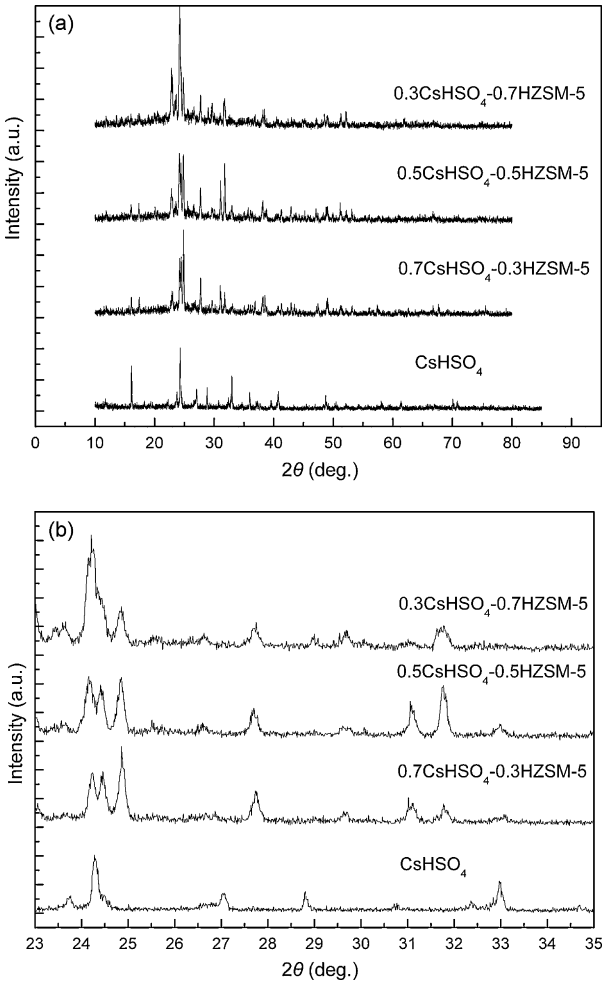

Fig. 2. XRD patterns of $CsHSO_4$–HZSM-5 composite membranes with different HZSM-5 contents.

electrolyte membrane was sandwiched between the graphite electrodes, and the copper sheets were placed outside the graphite electrodes to collect electronic signals for the impedance analyzer. A working electrode (WE) and sense electrode (SE) were placed on one side and a counter electrode (CE) and reference electrode (RE) were placed on the other. The heaters were placed outside of the copper sheets, and the thermocouple (TC) was placed in a slot in the graphite electrode, near the copper sheet side. The testing cell was fixed by bolt. The impedance was measured stepwise from 70 to 180 °C in static air.

3. Results and discussion

3.1. Structure analysis

The X-ray diffraction patterns of pure CHS and $(1-x)$CHS–xHZSM-5 composite electrolytes are shown in Fig. 2(a) (Si/Al = 35 for all the XRD samples, CZ37 means x = 0.7 in the $(1-x)$CHS–xHZSM-5 composite, i.e., 0.3CHS–0.7HZSM-5, CZ55 means x = 0.5, and likewise). The XRD pattern indicated that the prepared CHS was of a monoclinic structure and $P2_1/c$ (14) space group, which agreed with the previous report [3,8]. The unit cell parameters were a = 7.8147 Å, b = 8.1183 Å, c = 7.6892 Å, volume = 456.99 $Å^3$, and β = 110.5°. In comparison, the reflection peaks of CHS–HZSM-5 composite electrolytes were broadened and some new weak X-ray reflections appeared. The reason could be that the extremely small particles in the composites may give rise

Table 1
Crystallographic parameters (Å) of $(1-x)$CHS–xHZSM-5 (x = 0.3, 0.5, and 0.7) in the low-temperature phase.

Sample	a (Å)	b (Å)	c (Å)	β (°)	Volume (Å^3)	Space group	Crystal system
CHS	7.8147	8.1183	7.6892	110.5	456.99	$P21/c$ (14)	Monoclinic
CZ73	7.5441	8.1460	7.4529	108.3	434.87	$P21/c$ (14)	Monoclinic
CZ64	7.6490	8.4950	7.2237	109.0	443.61	$P21/c$ (14)	Monoclinic
CZ55	7.6390	8.4334	7.3128	108.99	445.48	$P21/c$ (14)	Monoclinic
CZ37	7.6711	8.4641	7.2233	108.82	443.93	$P21/c$ (14)	Monoclinic

to stronger interfacial interaction between the phases, which leads to a change in the bulk properties of the ionic salts [13]. In this case, the new phases may be stabilized at the CHS–HZSM-5 interface, which was similar with CHS–SiO_2 nanocomposites [8]. From Fig. 2(b), it can be observed that the intermediate-temperature phase of $CsHSO_4$ (phase II) formed in the CHS–HZSM-5 composite electrolyte. [14]. An additional reflection at $2\theta = 24.8°$ also appeared, which corresponds to the superprotonic phase (phase I) [6]. For CHS, phase II and phase III all are of monoclinic structure. However, the unit cell parameters of phase II are smaller than those of phase III, i.e., the distance between the nearest HSO_4^- groups is smaller in phase III than in phase II. As a result, the protons in phase II do not influence each other and thus vibrate independently [15–17]. Phase III of CHS usually transforms into phase II at 76 °C [15]. Phase II and phase I appeared in the CHS–HZSM-5 composite electrolyte and may be beneficial for proton transfer.

The crystallographic parameters of CHS–HZSM-5 composites are listed in Table 1. All the composites possessed a monoclinic structure, a $P21/c$ (14) space group, and the cell volumes of all the composites decreased after doping HZSM-5 particles. The decreased volumes agreed with the formation of phase II and phase I. Compared with the pure CHS, the a-axis and c-axis shortened and the b-axis increased in the CHS–HZSM-5 composites. For phase III of CHS, the zigzag chains of hydrogen bonds run along the b-axis of the crystal-linking SO_4 tetrahedra, which is along the a-axis for phase II and the c-axis for phase I [15]. The longer b-axis may be beneficial for low-temperature proton transfer.

3.2. Proton conductivity

Solid acid compounds like $CsHSO_4$ undergo a superprotonic phase transition at an intermediate temperature (T_{tr} = 141 °C). At this temperature, phase II of CHS transforms into phase I [18,19]. The crystal structure of phase I is tetragonal, $I4_1/amd$, and in phase I each SO_4 tetrahedra can adopt not one (as in phase III) but four crystallographically equivalent orientations, which means that the number of possible positions is larger than the number of protons, leading to high proton conductivity [15]. The heterogeneous dopant porous structure of CHS can enhance proton conductivity at low temperatures (<141 °C) [9]. The temperature dependency of the proton conductivity of $(1-x)CsHSO_4$–xHZSM-5 (Si/Al = 35) (CHS–HZSM-535) composite electrolytes is shown in Fig. 3. All the samples showed a superprotonic conductivity transition when the temperature increased. The doping HZSM-535 (Si/Al = 35) powders in the CHS electrolyte increased the proton conductivity in the low-temperature range. However, the conductivity at high temperatures (>140 °C) was lower than that of the pure CHS electrolyte, except for the sample of 0.6CHS–0.4HZSM-535. These results are similar to those of reported CHS doped with SiO_2 or TiO_2 [8,13].

It can also be seen that doping nanometer HZSM-535 powders in CHS electrolyte expanded the superprotonic phase transition range of CHS down to 100 °C. The change in the conductivity curves of CHS–HZSM-535 composite electrolytes was quite smooth when the HZSM-535 content increased. The effects of adding HZSM-535 may be related to its strong acidity. The formation of phase II in CHS–HZSM-5 may contribute to the higher conductivity at a low

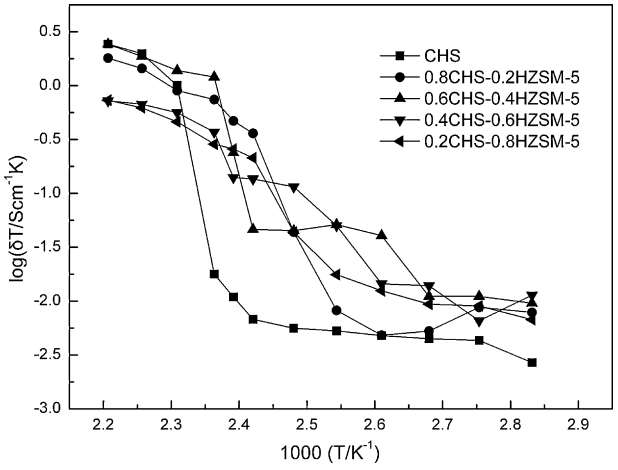

Fig. 3. Temperature dependence of the proton conductivity for CHS–HZSM-535 composite membranes with different HZSM-5 contents.

temperature [19]. Furthermore, the increase in the b-axis value of the CHS–HZSM-5 composite is beneficial for proton transfer in the low-temperature range because the protons move along the b-axis in low-temperature phase and a longer b-axis means the distance between the nearest HSO_4^- groups is larger. The protons therefore do not influence each other and instead vibrate independently, which facilitates proton transfer [15]. It has been suggested that the enhanced conductivity may be due to the formation of an interface phase between $CsHSO_4$ and HZSM-5 particles, i.e., structural disorder of $CsHSO_4$ in the interface phase occurs and contributes to the significant increase in proton conductivity in the low-temperature region [14,20].

The conductivity of 0.6CHS–0.4HZSM-535 composite electrolyte was measured stepwise between 70 and 180 °C in a heating–cooling cycle (Fig. 4). The high-temperature conductivities were almost the same in the heating and cooling processes. However, the low-

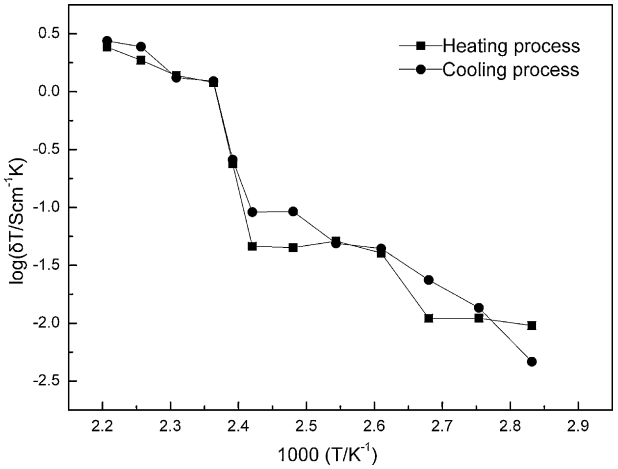

Fig. 4. Temperature dependence of the proton conductivity of 0.6CHS–0.4HZSM-535 composite membrane in a heating–cooling cycle.

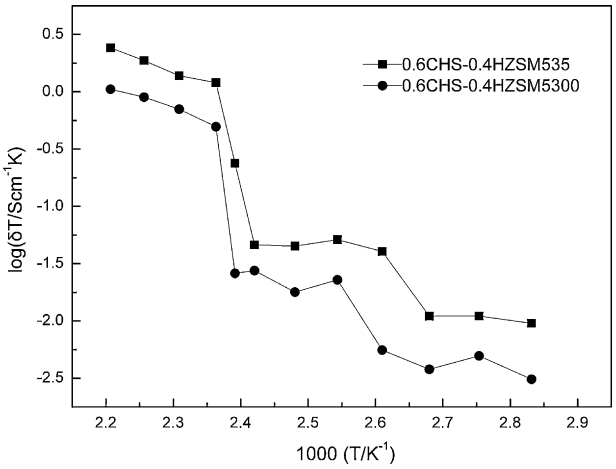

Fig. 5. Temperature dependence of the proton conductivity of 0.6CHS–0.4HZSM-535 and 0.6CHS–0.4HZSM-5300 composite membranes.

temperature conductivity in the cooling process showed a little higher than that in the heating process. The proton conductivity rapidly increased or decreased at about 130 °C in the heating and cooling processes, respectively. The results indicated that superprotonic phase transition reversibly occurred at 130 °C.

Ponomareva et al. [6] reported that the properties of CHS–SiO_2 composites could be defined by a special area, the character of the heterogeneous dopant porous structure, the pore radius, and so on. In the present study, we also examined the effect of different Si/Al ratios (35 and 300) of HZSM-5 on the conductivity of CHS–HZSM-5 composite electrolyte. The results are showed in Fig. 5. A similar tendency was observed in 0.6CHS–0.4HZSM-5300 (Si/Al = 300) composite electrolyte, which also showed superprotonic phase transition at about 130 °C. The conductivities of HZSM-5300 were about half an order lower than that of a HZSM-535 system in both the low- and the high-temperature regions, i.e., the conductivity decreased when the Al content increased. The results agreed with Ponomareva's that the conductivity of Al_2O_3-doped CHS composite electrolyte was lower than that of SiO_2-doped CHS [9].

3.3. Activation energy of the CHS–HZSM-5 composites

For $CsHSO_4$ solid acid electrolyte, proton transport is thought to take place through reorientation of the SO_4 tetrahedron and transfer between neighboring tetrahedrons along a hydrogen bond [1]. It was also acknowledged that two types of diffusion exist—one is the fast reorientation of HSO_4^- defects and the other is the slow long-range translational proton diffusion [21]. In the present work, we have investigated the proton transfer dynamics of CHS–HZSM-5 composite in high- and low-temperature regions.

The activation energies (E_a) of the CHS–HZSM-5 composite electrolyte can be derived from the Arrhenius equation (Eq. (1)):

$$\delta = A_0 T^{-1} \exp(E_a K^{-1} T^{-1}) \quad (1)$$

where A_0 is the pre-exponential factor, T is the absolute temperature, E_a is the activation energy for small polaron hopping, and K is the Boltzmann constant. The slope of the $\log \delta T$ vs. $1000/T$ data is the activation energy of the CHS–HZSM-535 composite electrolytes (see Table 2). The E_a value of pure CHS was calculated to be 34.1 kJ mol^{-1} in the high-temperature region and 26.4 kJ mol^{-1} in the low-temperature region. These results were similar to the data reported in the literature, where $E_a = 35 \pm 3$ kJ mol^{-1} and 29 kJ mol^{-1} in the high- and low-temperature regions, respectively [22,23]. The activation energy values of 0.6CHS–0.4HZSM-535 are given in Table 2. The high-temperature activation energy was

Table 2
Activation energies of proton conduction, E_a, in the $CsHSO_4$–HZSM-535 composites.

Sample	High-temperature region (kJ mol^{-1})	Low-temperature region (kJ mol^{-1})	References
Pure $CsHSO_4$	34.1	26.4	
0.6CHS–0.4HZSM-535	45.8	51.2	
CHS–SiO_2 (R70)	–	57.8	[5,8]
CHS–SiO_2 (R170)	–	91.5	[5,8]
Phase I in CHS	35	–	[21]
Phase II in CHS	–	29	[21]

45.8 kJ mol^{-1}, which was higher than that of the pure CHS electrolyte. This may be due to that the incorporation of HZSM-5 partly blocked the proton transfer path, making it more difficult for the proton transfer. The low-temperature E_a was 51.2 kJ mol^{-1}, about two times higher than that of pure CHS. However, the conductivity of CHS–HZSM-535 composite was higher than that of pure CHS, indicating that the proton transfer mechanism of CHS–HZSM-535 composite was different from that of the pure CHS at low temperatures. The amorphous phase in the composite electrolyte may contribute to the faster proton diffusion. For the heterogeneous doping composite electrolytes, the low-temperature E_a of the CHS–SiO_2 composite was 57.8 ± 4.8 kJ mol^{-1} when the pore radius was 70 Å (R70) and 91.5 kJ mol^{-1} for the sample with a pore radius of 170 Å (R170) [6,9]. The result indicates that the proton diffusion in the CHS–HZSM-535 composite can occur more easily than in CHS–SiO_2 composite [6,9].

3.4. Thermal analysis

The differential scanning calorimetry (DSC) curves for $(1-x)CsHSO_4$–xHZSM-5 (Si/Al = 35) composite electrolytes with different HZSM-5 contents are presented in Fig. 6. Pure CHS and CHS–HZSM-5 composite electrolytes exhibited two intense endothermic peaks from 300 to 600 K, which correspond to the phase transition (about 414 K) and melting process (about 450–480 K), respectively. The two CHS peaks agreed with the literature data [3]. The first peak (T = 414 K) corresponds to the phase transition from phase II to phase I, and the second one (T = 485 K) corresponds to the transition from phase I to liquid phase (melting process). The intensity of the phase transition peaks of the CHS–HZSM-5 composites decreases as HZSM-5 content increased. The melting peaks were broadened significantly, and the melting points of the CHS–HZSM-5 composites decreased with increasing the HZSM-5 content. This trend is similar to Ponomareva's

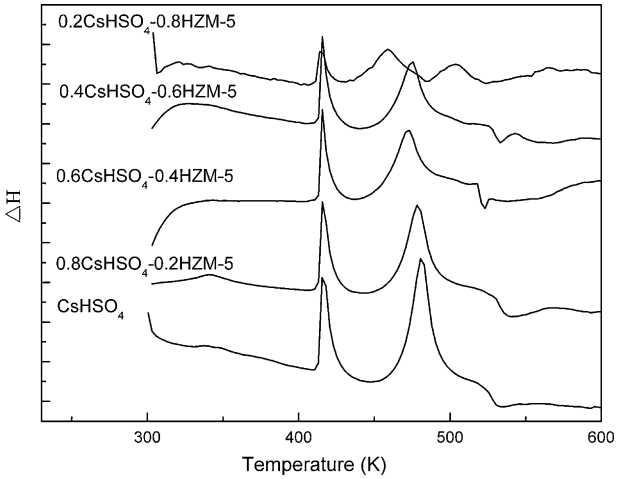

Fig. 6. DSC curves of $(1-x)CsHSO_4$–xHZSM-5 composites with different HZSM-5 contents.

results [6,8]. The phenomenon can be explained by considering the presence of the amorphous CHS in the CHS–HZSM-5 composites [6].

4. Conclusions

In this work, we prepared $CsHSO_4$–HZSM-5 composite electrolyte membranes for intermediate-temperature PEMFCs. The incorporation of the nanometer HZSM-5 powders into $CsHSO_4$ yielded significant effects on the crystalline structure, proton conductivity and thermal properties of the $CsHSO_4$ electrolyte. The proton conductivity was significantly increased at low temperatures in the composites. This improvement can be attributed to the change in the crystalline structure and the enhanced interfacial interaction between the two phases, which was conferred by compositing the extremely small HZSM-5 particles into CHS. The low-temperature activation energy of the composite with 40 mol% HZSM-5 was lower than that of the reported CHS–SiO_2 composite. This indicates that proton diffusion in CHS–HZSM-535 composite can occur more easily than that in the CHS–SiO_2 composite. Furthermore, thermal analysis results suggested that the melting point of the CHS–HZSM-5 composite electrolyte was lower than that of the pure CHS electrolyte. The $CsHSO_4$–HZSM-5 composite electrolyte is promising for application in PEMFCs operated at 100–200 °C.

In the future work, we will prepare the membrane electrode assembly using the prepared composite membrane, as well as investigate its performance in a single fuel cell and its long-term stability at high operating temperatures.

Acknowledgements

This investigation was supported by the National Nature Science Foundation of China (Project Nos. 20476034, 20876062) and the China Postdoctoral Science Foundation (Project Nos. 20080430826, 200801250).

References

[1] S.Q. Wang, J. Otomo, M. Ogura, C.J. Wen, H. Nagamoto, H. Takahashi, Solid State Ionics 176 (2005) 755–760.
[2] P. Bocchetta, R. Ferraro, F.D. Quarto, J. Power Sources 187 (2009) 49–56.
[3] P. Bocchetta, G. Chiavarotti, R. Masi, C. Sunseri, F.D. Quarto, Electrochem. Commun. 6 (2004) 923–928.
[4] S.M. Haile, D.A. Boysen, C.R.I. Chisholm, R.B. Merle, Nature 410 (2001) 910–913.
[5] M. Tatsumisago, T. Tezuka, A. Hayashi, K. Tadanaga, Solid State Ionics 176 (2005) 2909–2912.
[6] V.G. Ponomareva, G.V. Lavrova, L.G. Simonova, Solid State Ionics 118 (1999) 317–323, 220.
[7] V.G. Ponomareva, E.S. Shutova, Solid State Ionics 178 (2007) 729–734.
[8] V.G. Ponomareva, N.F. Uvarov, G.V. Lavrova, E.F. Hairetdinov, Solid State Ionics 90 (1996) 161–166.
[9] V.G. Ponomareva, G.V. Lavrova, Solid State Ionics 145 (2001) 197–204.
[10] B. Yang, A.M. Kannan, A. Manthiram, Mater. Res. Bull. 38 (2003) 691–698.
[11] J.D. Kim, T. Mori, T. Kudo, I. Honma, Solid State Ionics 179 (2008) 1178–1181.
[12] X. Zhao, H.M. Xiong, W. Xu, J.S. Chen, Mater. Chem. Phys. 80 (2003) 537–540.
[13] V.G. Ponomaevra, G.V. Lavrova, Solid State Ionics 106 (1998) 137–141.
[14] J. Otomo, S. Wang, H. Takahashi, H. Nagamoto, J. Membr. Sci. 279 (2006) 256–265.
[15] A.V. Belushkin, M.A. Adams, S. Hull, L.A. Shuvalov, Solid State Ionics 77 (1995) 91–96.
[16] C.R.I. Chisholm, S.M. Haile, Mater. Res. Bull. 35 (2000) 999–1005.
[17] T. Uda, D.A. Boysen, S.M. Haile, Solid State Ionics 176 (2005) 127–133.
[18] A.I. Baranov, L.A. Shuvalov, N.M. Shchagina, JETP Lett. 36 (1982) 459–462.
[19] A.V. Belushkin, R.M. Ibberson, L.A. Shuvalov, J. Mol. Struct. 374 (1996) 161–169.
[20] V.G. Ponomareva, G.V. Lavrova, L.G. Simonova, Solid State Ionics 118 (1999) 317–323.
[21] A.V. Belushkin, R.L. McGreevy, P. Zetterstrom, L.A. Shuvalov, Physica B 241–243 (1998) 323–325.
[22] S. Hayashi, M. Mizuno, Solid State Ionics 171 (2004) 289–293.
[23] M. Mizuno, S. Hayashi, Solid State Ionics 167 (2004) 317–323.